Supporting Information

Chou et al. 10.1073/pnas.1211175109

SI Materials and Methods

Cell Culture. Stromal and fibroblast lines were cultured in fibroblast growth media consisting of DMEM (Mediatech), 10% FBS, 2 mM glutamine (Invitrogen), 1% penicillin/streptomycin (Gibco), 100 μM nonessential amino acids (NEAAs, Invitrogen), 0.1 mM β-mercaptoethanol (BME), and 4 ng/mL bFGF (Invitrogen). Mononuclear cells (MNCs) were cultured in QBSF-60 media (Quality Biological) supplemented with stem cell factor (SCF) 100 ng/mL, thrombopoietin (TPO) 50 ng/mL, FLT3-ligand (FLT3L) 50 ng/mL, IL-3 10 ng/mL, and 1% penicillin/streptomycin (Gibco). Human ES cell (hES) media consisted of DMEM/F12 50/50 (Mediatech), 20% knockout serum replacement (Invitrogen), 2 mM L-glutamine, 1% penicillin/streptomycin, 100 μM NEAAs, 0.1 mM BME, and 10 ng/mL bFGF. All iPSC lines were maintained with hES cell media and on irradiated mouse embryonic fibroblasts (MEFs). Cultures were split weekly after incubation with TrypLe (Invitrogen) for 3–5 min and then mechanically disaggregated and plated on fresh MEFs.

Generation and Maintenance of Induced Pluripotent Stem Cells. To reprogram fibroblasts and stromal cells, 40,000 cells were transduced with 250 microliters of each pMXs-based retroviral supernatant with human *OCT4*, *SOX2*, *KLF4*, or *MYC* in six-well culture dishes in the presence of 5 mcg/mL polybrene and repeated 24 h later. For reprogramming mononuclear cells, 200,000 cells were infected with 5 μL each of concentrated pHage2-CMV-RTTA-W and pHage-Tet-hSTEMMCA-loxP virus in the presence of 5 mcg/mL polybrene, and spinoculated at 2,250 rpm at 25 °C for 1.5 h. One-half of the media was replaced after infection. Twenty-four hours later, cells were resuspended in fresh media with 1 mcg/mL doxycycline. Cells were split onto irradiated MEFs 3–6 d after infection and colonies were picked 21–28 d after infection and expanded. After 10 d, media was switched to hES cell media. Doxycycline was removed after colonies appeared.

Flow Cytometry. Antibodies used: anti-CD43 FITC, CD41a PE, CD42a FITC, CD235a APC, CD18 APC, CD34 PE-Cy7, Tra-1.60 FITC, Tra-1.81 AF555 (BD Biosciences); CD31 PE-Cy7, CD45 Pacific blue, SSEA3 AF488, SSEA4 AF647 (Biolegend); VEGFR2/KDR PE (R&D); CKIT (Invitrogen). Cells were stained as previously described (1), analyzed on a FacsCanto (BD Biosciences) with FloJo software (Tree Star), or sorted on a FACSAria (BD Biosciences).

Teratoma Assay. For teratoma formation, 1-million feeder-depleted induced pluripotent stem cells (iPSCs) were resuspended in 1:6 Matrigel (BD Biosciences) diluted in IMDM and injected intramuscularly into nonobese diabetic/severe combined immunodeficient mice. Teratomas were harvested 6–8 wk later and paraffin sections were stained with H&E. Animal experiments were performed in accordance with institutional guidelines at the Children's Hospital of Phildadelphia.

Karyotyping. Karyotyping of iPSCs was performed at the Coriell Institute of Medical Research (Camden, NJ).

Preparation of Cells from Embryoid Bodies. To assay embryoid bodies (EB), suspension cells were collected from the supernatant by harvesting EB cultures and centrifuging at 84 × *g* for 1 min. To analyze total EB cultures, EBs were dissociated to single cells by a 1-h incubation with 0.2% Collagenase B containing 20% serum followed by a 2-min incubation with trypsin (0.05% trypsin-EDTA) at 37 °C. After enzymatic treatment, 1 mL serum was added and the EBs were disaggregated to single cells by multiple passages through a 20-gauge needle.

Morphologic Analysis. Cells were centrifuged onto a glass slide and stained with May–Grunwald-Giemsa (Sigma). Light microscopy images were obtained with a Zeiss Axioskope 2 microscope, Axiocam camera, and AxioVision 4.8 software (Carl Zeiss Microimaging).

Semiquantitative Real-Time PCR Primers Used. Cyclophilin: F′ GAA GAG TGC GAT CAA GAA CCC ATG AC, R′ GTC TCT CCT CCT TCT CCT CCT ATC TTT ACT T; DNMT3B: F′ TAC AGA CGT GTG CAG TTG TAG GCA, R′ GTG CAG ACT CCA GCC CTT GTA TTT; REX1: AAA GCA TCT CCT CAT TCA TGG T, R′ TGG GCT TTC AGG TTA TTT GAC T; ABCG2: TCA GGA GAC CAC ATT TCA TCT AGC CC, R′ CAG GGC ACC CAC TGA CAA ACT AAA; NANOG: F′ CCT GAA GAC GTG TGA AGA TGA G, R′ GCT GAT TAG GCT CCA ACC ATA C; α-globin: F′ ACG GTG CTG ACC TCC AAA TAC C, R′ GCC GCC CAC TCA GAC TTT ATT CA; β-globin: F′ GGA TCT GTC CAC TCC TGA TGC TGT T, R' CCC TTG AGG TTG TCC AGG TGA G; ε-globin: F′ GCT GCA ATC ACT AGC AAG CTC TCA; R′ TTC ACC TCC AGC CTC TTC CAC ATT CA; γ-globin: F′ AGC AGT TCC ACA CAC TCG CTT CT, R′ TCT CCT CCA GCA TCT TCC ACA TTC AC; ζ-globin: F′ ACC AAG ACC TAC TTC CCG CAC TT, R' CGA TGT CGT CGA TGC TCT TCA CC. For expression of lentivirus transgene OCT4-KLF4: F′ GGT GCG CCA GTA AAG CAG ACA TTA AA, R′ CAG ACG CGA ACG TGG AGA AAG A. For expression of the retrovirus transgenes: RETRO: F′-CCC TCA AAG TAG ACG GCA TC; RETRO_OCT: R′ GCG AGA AGG CAA AAT CTG AA; RETRO_SOX R′: TTC AGC TCC GTC TCC ATC AT; RETRO_KLF R′: GTG GAG AAA GAT GGG AGC AG; RETRO_MYC R′: AGG CTG CTG GTT TTC CAC TA.

Microarray and Bioinformatic Analysis. To investigate differential expression, we performed a parametric two-sample Student *t* test on the whole set of 19,392 genes, comparing differences in mean expression of genes between T21 and euploid iPSC-derived progenitors. The resulting *P* values displayed an almost "flat" distribution across the spectrum of *P* values. Thus, a genome-wide analysis reveals very few genes, if any, that are differentially expressed between T21 and euploid cells. At a *P* value threshold of <0.05, the expected number of differentially expressed genes that could result from random fluctuation (false-positives) is 967 for a genome-wide comparison. Gene-dosage effects should be limited to chromosome 21, which has only 236 genes, and that is four-times lower than the number of false-positives expected for the genome-wide analysis. For this reason we decided to restrict our search for differentially expressed genes because of gene-dosage effects to those located on chromosome 21. This approach allowed a more sensitive selection of genes that show a clear gene dosage effect resulting from the presence of an additional copy of chromosome 21.

Restricting the Student *t* test to the 236 genes from the Affymetrix arrays that are on chromosome 21 revealed enrichment for genes at low *P* value. Next, we corrected the *P* values for multiple testing using Benjamini–Hochberg false-discovery rate (BH-FDR) method (2). Comparison of distributions of adjusted *P* values (FDR) coming from the genome-wide set, chromosome 21, as well as 100 sets of randomly chosen 236 genes, confirmed again that chromosome 21 is enriched for differentially expressed genes,

which further justified our decision to focus our analysis on chromosome 21 only. Following the application of BH-FDR threshold of <0.2, which resulted in 71 genes (Table S2), we applied a secondary threshold of ≥1.5-fold change in mean expression between T21 and euploid samples, corresponding to biologically predicted increase in gene expression resulting from the presence of an additional copy of chromosome 21. Twenty-one genes showed a clear dosage effect, suggesting that small changes in a number of genes on chromosome 21 are responsible for the hematopoietic phenotype we observed.

We also examined separately 38 genes outside of HSA21 (Table S2) that are known to play important roles in hematopoietic lineage determination and differentiation. For these 38 selected genes, we again performed a parametric two-sample Student *t* test and multiple testing correction using BH-FDR method. *P* values and FDR values for all 38 genes are reported in Table S2.

Mouse Models. TsDn65 mice were purchased from Jackson Laboratories. Genotyping was performed by a PCR screen for a single nucleotide polymorphism within the *Zdhhc14* gene using restriction enzyme digest of the PCR product amplified from embryo DNA, described in ref. 3. Embyronic day (E) 8.5 yolk sacs were dissected in Pb-1 buffer (4). E12.5 embryos were collected as previously described (5). Tissues were dissociated for 1 h at 37° in 0.125% collagenase type I (Sigma) in PBS with 10% FBS. Cells were cultured at 1/4 embryonic equivalents for yolk sac and 0.5% and 1% embryonic equivalents for fetal liver in M3434 (StemCell Technologies) for 7 d at 37 °C, 5% CO_2. Primitive colonies were scored on day 5 and definitive on day 7. Embryos were imaged with a Leica MZFIII stereomicroscope with a Plan 1× 0.14 objective lens (Leica) and a 11.2 Color Mosaic camera with Spot 4.0 acquisition software (Diagnostic Instruments).

1. Chou ST, et al. (2008) Trisomy 21 enhances human fetal erythro-megakaryocytic development. *Blood* 112(12):4503–4506.
2. Benjamini Y, Hochberg Y (1995) Controlling the false discovery rate—A practical and powerful approach to multiple testing. *J R Stat Soc, B* 57:289–300.
3. Lorenzi H, Duvall N, Cherry SM, Reeves RH, Roper RJ (2010) PCR prescreen for genotyping the Ts65Dn mouse model of Down syndrome. *Biotechniques* 48(1):35–38.
4. Monk M (1987) *Mammalian Development: A Practical Approach* (Oxford Univ Press, Oxford).
5. Kingsley PD, Malik J, Fantauzzo KA, Palis J (2004) Yolk sac-derived primitive erythroblasts enucleate during mammalian embryogenesis. *Blood* 104(1):19–25.

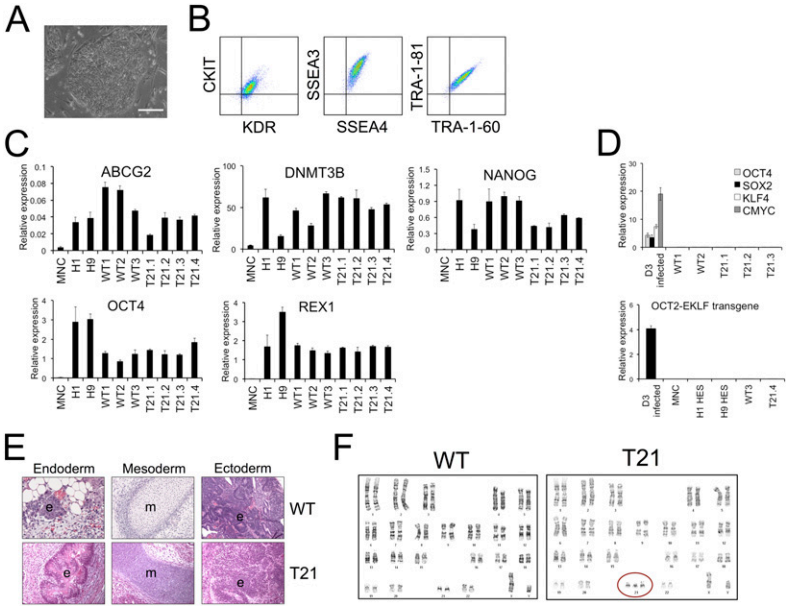

Fig. S1. Generation of trisomy 21 (T21) and euploid iPSCs. (*A*) Photomicrograph demonstrating morphology of representative iPSC colony. (Scale bar, 200 μm.) (*B*) Representative flow cytometric analysis of iPSCs for cell-surface expression of typical hES cell markers CKIT, KDR (VEGFR), SSEA3, SSEA4, TRA-1-81, and TRA-1-60. (*C*) Expression levels of endogenous factors quantified by semiquantitative RT-PCR (qRT-PCR) shown relative to cyclophilin levels. Results are shown as mean values ± SD. (*D*) Expression levels of transgenic factors determined by qRT-PCR relative to cyclophilin levels. Results are shown as mean values plus or minus SD. MNC, mononuclear cells, HES, human embryonic stem cell. (*E*) Representative photomicrographs of teratomas generated from euploid (WT) and T21 iPSCs injected into (NOD/SCID) beige mice contain all three germ layers. Letters (e, m, e) indicate corresponding germ layer: endoderm, mesoderm, ectoderm. Original magnification, 10×. (*F*) Representative karyotype analysis of iPSC clones.

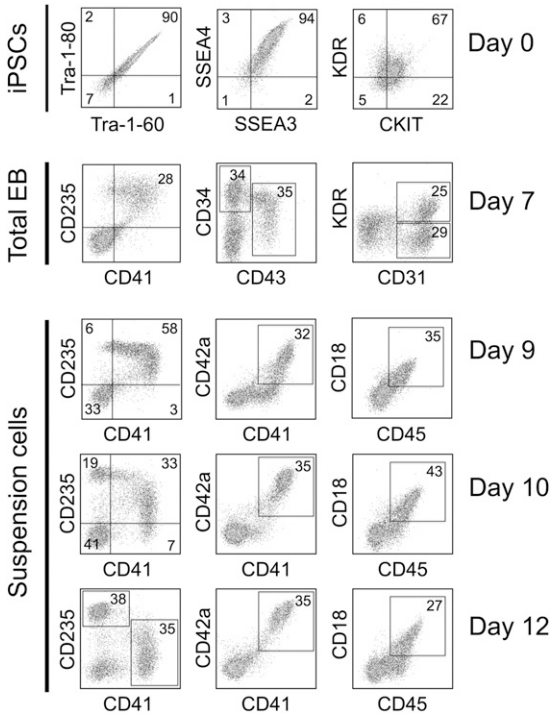

Fig. S2. Hematopoietic differentiation of iPSCs via EB formation. Representative cell-surface expression profiles of undifferentiated iPSCs on day 0, total EB cultures on day 7, and suspension cells released from EBs on days 9, 10, and 12 of differentiation, demonstrating progressive hematopoietic cell lineage commitment to erythroid ($CD41^{-}235^{+}$), megakaryocytic ($CD41^{+}42^{+}$), and myeloid ($CD45^{+}18^{+}$) cells.

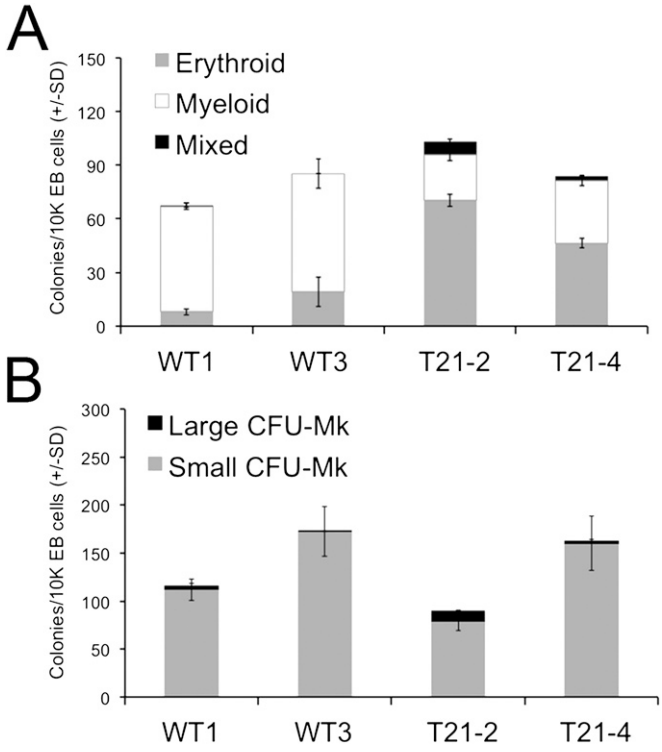

Fig. S3. Increased erythroid progenitors in trisomy 21 induced pluripotent stem cell differentiation cultures from total EBs. (*A*) Methylcellulose colony assays containing SCF, IL-3, EPO, and GM-CSF, and (*B*) colony-forming megakaryocyte (CFU-Mk) assays containing TPO, IL-3, and IL-6 of disaggregated embryoid bodies on day 7–8 of EB differentiation from T21 and euploid iPSCs. Results show mean values ± SD, $n = 2$ per group.

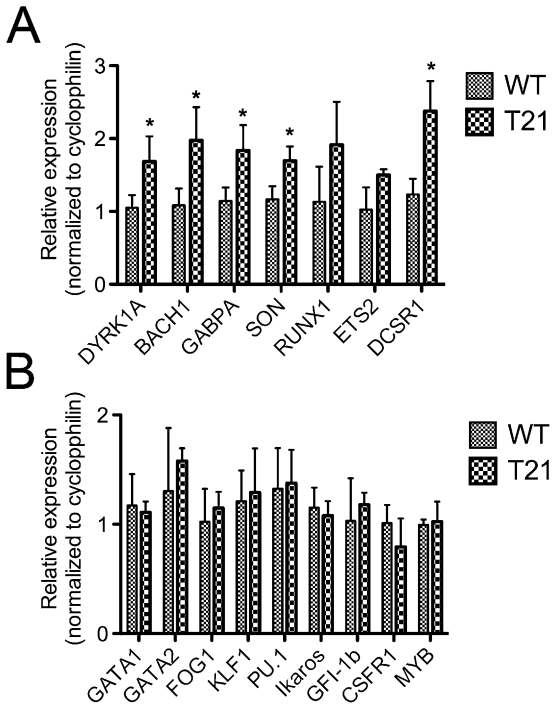

Fig. S4. Expression of key hematopoietic regulators in iPSC-derived progenitors. (*A*) Expression of chromosome 21-encoded hematopoietic transcription factors by qRT-PCR in purified WT and T21 iPSC-derived hematopoietic progenitors. $n = 3$ per group. *P values < 0.05. (*B*) Expression of key hematopoietic regulators by RT-PCR in WT and T21 iPSC-derived hematopoietic progenitors. $n = 3$ per group. Results are shown as mean ± SEM.

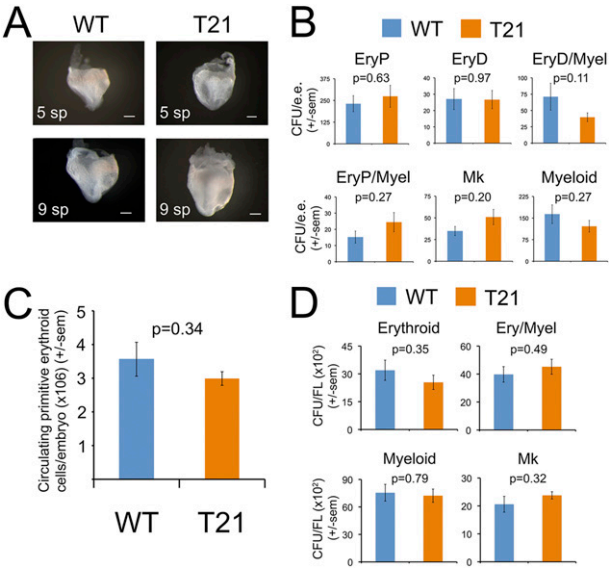

Fig. S5. Normal primitive and definitive hematopoiesis in the Ts65Dn murine model for Down syndrome. (*A*) Photographic representation of E8.5 WT and T21 yolk sacs at five and nine somite-pair (sp) stages. (Scale bars, 200 μm.) (*B*) Methylcellulose colony assays of WT and T21 yolk sac-derived cells. Results are shown as mean CFUs per WT ($n = 6$) or T21 ($n = 9$) embryonic equivalent ± SEM. EryP, primitive erythroid, EryD, definitive erythroid, Mk, megakaryocyte. EryP/Myel indicates primitive erythroid colony with macrophages and megakaryocytes. EryD/Myel indicates burst-forming unit-erythroid with macrophages, granulocytes, and megakaryocytes. (*C*) Circulating primitive erythroid cell counts in WT ($n = 7$) and T21 ($n = 6$) E12.5 embryos. Results are shown as mean ± sem. (*D*) Methylcellulose colony assays of WT and T21 fetal liver-derived cells from E12.5 embryos. Results are shown as mean CFU per wild type ($n = 7$) or T21 ($n = 7$) fetal liver ± SEM. Ery/myel, erythroid/myeloid.

Table S1. Induced pluripotent stem cell lines generated and analyzed

iPSC line	Cell of origin	Reprogramming method	Karyotype
WT1*	Neonatal fibroblast	Retrovirus: OSKM	46, XY
WT2	Fetal stromal cell	Retrovirus: OSKM	46, XY
WT3	Fetal mononuclear cell	Lentivirus: OSKM	46, XY
T21.1	Neonatal fibroblast	Retrovirus: OSKM	47, XY, +21
T21.2	Fetal stromal cell	Retrovirus: OSKM	47, XY, +21
T21.3	Fetal stromal cell	Retrovirus: OSKM	47, XY, +21
T21.4	Fetal mononuclear cell	Lentivirus: OSKM	47, XY, +21

Reprogramming was performed either by using a combination of four separate pMXs-based retroviruses, each encoding *OCT4*, *SOX2*, *KLF4*, or *MYC*, or by a single polycistronic lentiviral vector encoding all four genes regulated by a doxycycline inducible promoter. T21, trisomy 21; WT, wild-type (euploid).
*Line purchased from laboratory of George Daley (Boston, MA).

Table S2. T21 vs. euploid expression of selected genes in iPSC-derived progenitors

Gene symbol	Chromosome	Fold-change	*P* value	FDR
71 differentially expressed Chromosome 21 genes (FDR < 0.2)				
N6:00 AMT1	chr21	1.97 (+)	0.0335	0.15
C21orf91	chr21	1.89 (+)	0.0071	0.07
GART	chr21	1.84 (+)	0.0005	0.06
C21orf57	chr21	1.70 (+)	0.0480	0.19
IFNAR2	chr21	1.68 (+)	0.0291	0.14
*SH3BGR**	chr21	1.66 (+)	0.0050	0.07
HSPA13	chr21	1.66 (+)	0.0093	0.08
*BRWD1**	chr21	1.64 (+)	0.0287	0.14
URB1	chr21	1.63 (+)	0.0014	0.06
IFNAR1	chr21	1.61 (+)	0.0237	0.12
*DSCR3**	chr21	1.60 (+)	0.0579	0.19
ADARB1	chr21	1.60 (+)	0.0559	0.19
TMEM50B	chr21	1.60 (+)	0.0177	0.10
*MORC3**	chr21	1.55 (+)	0.0024	0.06
MCM3AP-AS	chr21	1.55 (+)	0.0311	0.15
*BACE2**	chr21	1.54 (+)	0.0136	0.09
*HLCS**	chr21	1.54 (+)	0.0141	0.09
CYYR1	chr21	1.53 (+)	0.0089	0.08
*WRB**	chr21	1.52 (+)	0.0041	0.07
DNAJC28	chr21	1.51 (+)	0.0332	0.15
BACH1	chr21	1.50 (+)	0.0313	0.15
DONSON	chr21	1.49 (+)	0.0207	0.11
PRMT2	chr21	1.49 (+)	0.0327	0.15
UBE2G2	chr21	1.47 (+)	0.0126	0.09
C21orf45	chr21	1.45 (+)	0.0500	0.19
U2AF1	chr21	1.45 (+)	0.0180	0.10
MCM3AP	chr21	1.45 (+)	0.0003	0.06
GCFC1	chr21	1.44 (+)	0.0028	0.06
RRP1	chr21	1.43 (+)	0.0520	0.19
TIAM1	chr21	1.43 (+)	0.0330	0.15
USP25	chr21	1.43 (+)	0.0063	0.07
LTN1	chr21	1.43 (+)	0.0013	0.06
CRYZL1	chr21	1.40 (+)	0.0008	0.06
FAM165B	chr21	1.40 (+)	0.0076	0.07
C21orf59	chr21	1.40 (+)	0.0058	0.07
NRIP1	chr21	1.39 (+)	0.0065	0.07
SLC5A3	chr21	1.39 (+)	0.0172	0.10
*TTC3**	chr21	1.39 (+)	0.0091	0.08
CBS	chr21	1.38 (+)	0.0033	0.06
NDUFV3	chr21	1.37 (+)	0.0025	0.06
LSS	chr21	1.37 (+)	0.0565	0.19
TRAPPC10	chr21	1.36 (+)	0.0456	0.18
IFNGR2	chr21	1.35 (+)	0.0051	0.07
*PIGP**	chr21	1.35 (+)	0.0288	0.14
*DYRK1A**	chr21	1.34 (+)	0.0027	0.06
ATP5J	chr21	1.31 (+)	0.0156	0.10
USP16	chr21	1.31 (+)	0.0018	0.06
PCNT	chr21	1.30 (+)	0.0062	0.07
PTTG1IP	chr21	1.30 (+)	0.0173	0.10
ATP5O	chr21	1.30 (+)	0.0016	0.06
GABPA	chr21	1.29 (+)	0.0023	0.06
SFRS15	chr21	1.29 (+)	0.0382	0.16
*PSMG1**	chr21	1.27 (+)	0.0066	0.07
PWP2	chr21	1.26 (+)	0.0504	0.19
SON	chr21	1.25 (+)	0.0141	0.09
SOD1	chr21	1.24 (+)	0.0126	0.09
*HMGN1**	chr21	1.22 (+)	0.0223	0.12
*SETD4**	chr21	1.22 (+)	0.0045	0.07
SUMO3	chr21	1.21 (+)	0.0573	0.19
C21orf33	chr21	1.21 (+)	0.0573	0.19
CSTB	chr21	1.21 (+)	0.0129	0.09
MRAP	chr21	1.20 (+)	0.0123	0.09

Table S2. Cont.

Gene symbol	Chromosome	Fold-change	*P* value	FDR
ABCC13	chr21	1.07 (+)	0.0508	0.19
ICOSLG	chr21	1.07 (–)	0.0144	0.09
TMPRSS3	chr21	1.12 (–)	0.0346	0.15
C21orf125	chr21	1.15 (–)	0.0355	0.15
MIR125B2	chr21	1.29 (–)	0.0554	0.19
KCNE1	chr21	1.33 (–)	0.0079	0.07
KRTAP10-6	chr21	1.34 (–)	0.0063	0.07
KRTAP12-4	chr21	1.35 (–)	0.0579	0.19
KRTAP10-4	chr21	1.53 (–)	0.0383	0.16
38 genes involved in hematopoietic lineage determination and differentiation				
KIT	chr4	1.54 (+)	0.4634	0.95
EPOR	chr19	1.23 (+)	0.1935	0.92
GATA2	chr3	1.20 (+)	0.1230	0.78
MYB	chr6	1.18 (+)	0.0003	0.01
CEBPB	chr20	1.10 (+)	0.2525	0.95
TFRC (CD71)	chr3	1.10 (+)	0.5248	0.95
IKZF1 (Ikaros)	chr7	1.07 (+)	0.6739	0.95
TAL1 (SCL)	chr1	1.07 (+)	0.7926	0.95
LMO2	chr11	1.06 (+)	0.3061	0.95
NOTCH1	chr9	1.06 (+)	0.4100	0.95
BMP4	chr14	1.06 (+)	0.4280	0.95
PHC1 (RAE28)	chr12	1.04 (+)	0.6536	0.95
HES1	chr3	1.04 (+)	0.8698	0.95
IL5	chr5	1.03 (+)	0.6221	0.95
ITGA2B (CD41)	chr17	1.03 (+)	0.8062	0.95
CBFB	chr16	1.02 (+)	0.7537	0.95
SPI1 (PU.1)	chr11	1.02 (+)	0.9308	0.95
TGFB1	chr19	1.01 (+)	0.9531	0.95
ZBTB7A (LRF)	chr19	1.01 (–)	0.9053	0.95
EPO	chr7	1.02 (–)	0.6805	0.95
CEBPA	chr19	1.02 (–)	0.8777	0.95
GYPA (CD235)	chr4	1.03 (–)	0.8600	0.95
KLF1	chr19	1.04 (–)	0.7328	0.95
CSF3R (G-CSF-R)	chr1	1.04 (–)	0.7516	0.95
GFI1B	chr9	1.05 (–)	0.5540	0.95
ZFPM1 (FOG1)	chr16	1.06 (–)	0.3857	0.95
TPO	chr2	1.07 (–)	0.4599	0.95
MLL	chr11	1.07 (–)	0.5979	0.95
GATA1	chrX	1.08 (–)	0.2710	0.95
CSF2RA	chrX	1.10 (–)	0.0622	0.57
FLT3 (FLK2)	chr13	1.12 (–)	0.3609	0.95
SPN (CD43)	chr16	1.13 (–)	0.1779	0.92
CSF1R (C-FMS)	chr5	1.19 (–)	0.0150	0.29
THY1 (CD90)	chr11	1.20 (–)	0.5170	0.95
FLI1	chr11	1.26 (–)	0.3032	0.95
BMI1	chr10	1.32 (–)	0.0753	0.57
KDR (FLK1)	chr4	1.51 (–)	0.5731	0.95
CD34	chr1	1.75 (–)	0.0443	0.56

The upper portion of the table shows 71 differentially expressed chromosome 21 genes (FDR < 0.2). The lower portion of table shows gene expression of 38 selected genes involved in hematopoietic lineage determination and differentiation. "Fold-change" reports the degree of up-regulation (+) or down-regulation (–) of mean gene expression in T21 with respect to euploid cells. *P* values were obtained from parametric two-sample Student *t* test comparing differences in mean expression between T21 and euploid cells. FDR values were obtained using the BH-FDR method.

*Denotes location within Down syndrome critical region.